Available online at www.sciencedirect.com
ScienceDirect
Acta Materialia 56 (2008) 5255–5262
Acta MATERIALIA
www.elsevier.com/locate/actamat

Vacancy thermodynamics for intermediate phases using the compound energy formalism ☆

W.A. Oates [a,*], S.-L. Chen [b], W. Cao [b], F. Zhang [b], Y.A. Chang [c], L. Bencze [d], E. Doernberg [e], R. Schmid-Fetzer [e]

[a] Institute for Materials Research, University of Salford, Salford M5 4WT, UK
[b] CompuTherm LLC, 437 S. Yellowstone Drive, Madison, WI 53719, USA
[c] Department of Materials Science and Engineering, University of Wisconsin, Madison, WI 53706, USA
[d] Department of Physical Chemistry, Roland Eötvös University, 1117 Budapest, Pázmány Péter sétány 2, Hungary
[e] Institute of Metallurgy, Clausthal University of Technology, D-38678, Clausthal-Zellerfeld, Germany

Received 20 October 2007; received in revised form 8 January 2008; accepted 2 July 2008
Available online 8 August 2008

Abstract

The compound energy formalism is widely used for thermodynamic descriptions of intermediate phases containing vacancies. For a two-sublattice model, represented by $(A,B,Va)_{0.5} : (A,B,Va)_{0.5}$, it is physically necessary to take the reference state Gibbs energy of the pure vacancy end member, $G^{o}_{Va:Va}$, as zero, irrespective of temperature, pressure, or the chemical composition and structure of the actual intermediate phase containing the vacancies. This assumption leads to more than one possible solution for the calculated value of the equilibrium vacancy concentration. The assumption can be avoided if the compound end members are regarded as cluster solution members and an ideal dilute solution reference state is used for the vacancy clusters. In this case, $G^{o}_{Va:Va}$ does depend on the host as well as on temperature and pressure. An analysis of the thermodynamic properties of the B2 phase in the Al–Ni system is used as a demonstration of this alternative view.

Keywords: Vacancies; Compound energy formalism; Thermodynamics; Chemical potential; Intermetallic compounds

1. Introduction

Vacancies are present at equilibrium in all metals and alloys but usually in such small concentrations that their presence can be ignored when describing the thermodynamic properties of a phase with an appropriate modeling equation. Occasionally, however, especially with some intermediate phases, B2-AlNi and B2-AlFe being the classic examples, vacancies are present in sufficiently high concentrations that they must be taken into account when arriving at a satisfactory thermodynamic description of the phase.

Vacancies are a unique thermodynamic component. Unlike chemical elements, it is not possible to control their external chemical potential nor is it possible for them to be considered in a materials balance. All that is available, experimentally, is one result, the equilibrium vacancy concentration at constant pressure, temperature, chemical composition and structure. Nevertheless, it is necessary to have some thermodynamic representation of this information so that it can be used in the thermodynamic modeling of metal- or alloy-vacancy systems.

The models used for treating vacancy thermodynamics in metals and alloys have varied in their approach. We first discuss two different approaches which have been used for

☆ This article was presented at the Symposium on Phase Stability and Defect Structures in Honor of Professor Austin Chang, held in Orlando, FL, February 28–March 2, 2007.

* Corresponding author. Tel.: +1 608 274 1414; fax: +1 608 274 6045.
E-mail addresses: aoates@globalnet.co.uk (W.A. Oates), chen@chorus.net (S.-L. Chen).

1359-6454/$34.00 © 2008 Acta Materialia Inc. Published by Elsevier Ltd. All rights reserved.
doi:10.1016/j.actamat.2008.07.002

pure metals since these serve to introduce the problem on which we wish to concentrate, namely vacancy thermodynamics in intermediate phases.

2. Vacancy thermodynamics in pure metals

We will first consider a thermodynamic analysis for a substitutional A–B alloy and then compare it with one for an A–Va alloy. We use X_s to refer to a thermodynamic quantity per mole of sites and X_a to refer to a quantity per mole of A atoms.

(a) A–B alloys

Consider a closed system for an A–B alloy. If the alloy is one comprising a single lattice only, there is no thermodynamic potential to be minimized. Given p, T, N_A, N_B, the properties of the system are fixed. If, however, the alloy phase contains sublattices, the Gibbs energy to be minimized in the closed system can be written $G([p, T, N_A, N_B], \eta)$, where the square bracketed terms are held constant whilst the other term(s) is(are) the independent variables. The minimization of G gives the equilibrium values of the internal variable(s), given here as a single long-range order parameter η.

Now consider an open system for an A–B alloy with a fixed number of A atoms. The system is open to the component B at a fixed μ_B, denoted by μ_B^R on the $x_B = 1$ ordinate in Fig. 1. A tangent can be drawn from the point μ_B^R to the G_s curve to give the equilibrium concentration. This method can be used for either single lattice or sublattice phases.

In using this method, the Gibbs energy is being minimized subject to the constraint that $\mu_B = \mu_B^R$. The appropriate thermodynamic potential which has an unconstrained minimum, i.e., reaches a minimum value at the equilibrium composition for fixed p, T, N_A, μ_B^R, is the quasi-grand potential, $\Omega([p, T, N_A, \mu_B^R], N_B)$. (The name grand potential is reserved for conditions of constant V, T, N_A, μ_B^R.) The quasi-grand potential is defined by:

$$\Omega = G - \mu_B^R N_B = \mu_A N_A + \mu_B N_B - \mu_B^R N_B$$

Since N_A is fixed we can write:

$$\frac{\Omega}{N_A} = \frac{G}{N_A} - \frac{N_B}{N_A}\mu_B^R$$

$$\Omega_a = G_a - \frac{x_B}{x_A}\mu_B^R \tag{1}$$

The relation between G_a and Ω_a for an ideal solution, i.e., for one where $G_a = \log_e x_A + \frac{x_B}{x_A}\log_e x_B$, is shown in Fig. 2. The minimum in Ω_a occurs where the difference $G_a - \frac{x_B}{x_A}\mu_B^R$ reaches its maximum absolute value. This is shown by the vertical arrow in the figure. This minimum value of Ω_a is equal to the equilibrium value of μ_A corresponding to the fixed value of μ_B^R.

(b) A–Va alloys

A–Va alloys differ from the A–B alloy in that the only experimental result available, at fixed p, T, N_A, is the equilibrium value of x_{Va}. There are no experimental results which permit the construction of an experimental G_s vs. x_{Va} curve similar to that which is possible for A–B alloys. It is not possible, experimentally, to maintain x_{Va} at a fixed value and measure or calculate the Gibbs energy for an A–Va system, nor is it possible, experimentally, to maintain μ_{Va} at a fixed value and minimize the quasi-grand potential.

Notwithstanding this experimental impossibility of controlling either x_{Va} or μ_{Va}, it is possible to carry out virtual experiments (or thought experiments or gedankenexperiments) via the use of a modeling equation. The only requirement of this modeling equation is that it should reproduce the equilibrium value of x_{Va}. Such virtual experiments permit the consideration of other, experimentally unattainable, x_{Va} or μ_{Va} values. Fig. 3 shows both G_a, where the minimum occurs and G_s, where the usual tangent/intercept rule for obtaining the constrained minimum can be applied. The particular curves

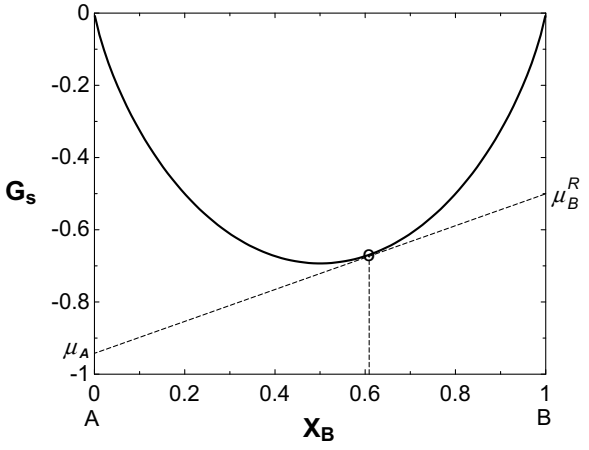

Fig. 1. Variation of the molar Gibbs energy, G_s, with x_B. If μ_B is fixed at the value shown, μ_B^R, the equilibrium value of x_B is obtained from the tangent to G_s.

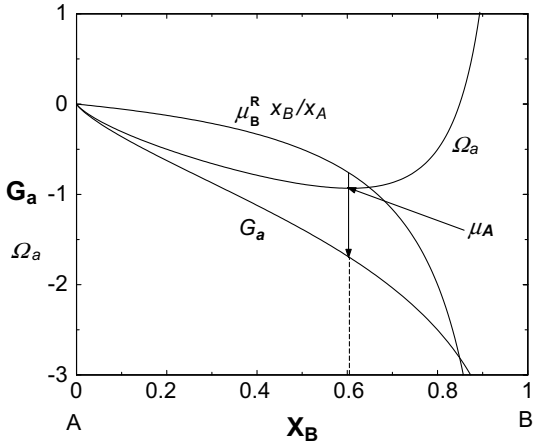

Fig. 2. Ω_a is the appropriate thermodynamic potential to be minimized for constant p, T, μ_B^R. Its relation to G_a and $\mu_B^R x_B/x_A$ is shown. The vertical arrow indicates the difference between these two quantities at the equilibrium composition. The minimum in Ω_a occurs at the equilibrium value of μ_A corresponding to μ_B^R.

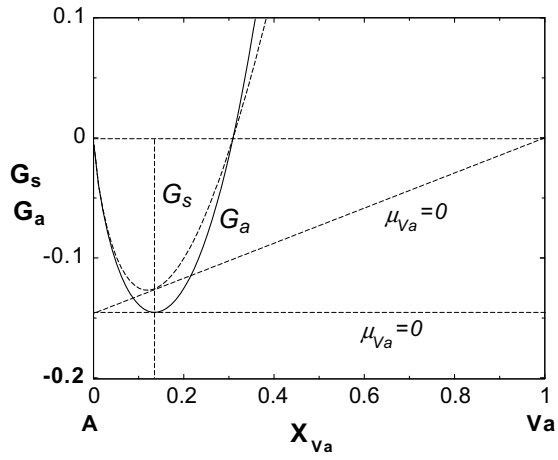

Fig. 3. G_s and G_a plotted as a function of x_{Va}. The minimum in G_a is seen to occur at the same value of x_{Va} as that obtained from the tangent to G_s where $\mu_{Va} = 0$.

shown have been drawn by assuming an ideal dilute solution for Va in A. An infinite number of different modeling equations could, however, also give the same equilibrium value of x_{Va} at the minimum in G_a, i.e., where

$$\left(\frac{\partial G}{\partial N_{Va}}\right)_{p,T,N_A} = \mu_{Va} = 0 \tag{2}$$

The large number of possible modeling equations can be grouped as originating from two different approaches:

2.1. First method

If the concentration of vacancies, x_{Va}, defined as $x_{Va} = N_{Va}/(N_M + N_{Va})$, and the ideal dilute solution approximation is used, then the vacancy chemical potential is given by:

$$\mu_{Va} = \mu^o_{Va} + RT\log_e(x_{Va}) \tag{3}$$

where μ^o_{Va} is the reference value for the vacancy chemical potential. Combination of Eqs. (2) and (3) gives the equilibrium vacancy concentration, x^{eq}_{Va}:

$$x^{eq}_{Va} = \exp(-\mu^o_{Va}/RT) \tag{4}$$

Since $0 \leqslant x^{eq}_{Va} \leqslant 1$, μ^o_{Va} must be positive. As indicated in the Section 1, x^{eq}_{Va} is the only piece of experimental information available and it follows that μ^o_{Va} is selected to give this equilibrium value. The analytical form given in Eq. (3) is suitable for representing the properties at other vacancy concentrations, at the standard pressure.

If the Gibbs energy per mole of sites, G_s, is defined as:

$$G_s = \frac{G}{N_M + N_{Va}} \tag{5}$$

then G_s in terms of the metal and vacancy chemical potentials is given by:

$$G_s = (1 - x_{Va})\mu_M + x_{Va}\mu_{Va} \tag{6}$$

$$G_s = (1 - x_{Va})\mu^o_M + x_{Va}\mu^o_{Va} + RT[(1 - x_{Va})\log_e(1 - x_{Va}) + x_{Va}\log_e x_{Va}] \tag{7}$$

Fig. 4 shows a plot of G_s, for the ideal dilute solution obtained from Eq. (7), vs. x_{Va}, for a hypothetical system with $\mu^o_{Va} = 21{,}280$ J mol^{-1} at 1000 K (μ^o_M has been taken to be zero). The tangent line to the curve at $x_{Va} = 0.0773$ (point "**a**") has an ordinate intercept of zero at $x_{Va} = 1$. This intercept corresponds with $\mu_{Va} = 0$. The minimum in G_s, shown in Fig. 4, which occurs at $x_{Va} = 0.0718$ (point "**b**"), is not the equilibrium state for $\mu_{Va} = 0$ but corresponds with the point where $\mu_{Va} = \mu_M$. The equilibrium state is given by the constrained ($\mu_{Va} = 0$) minimum in G_s at point "**a**".

Note that G_s is a convex function of x_{Va} over the whole range $0 \leqslant x_{Va} \leqslant 1$, so that the equilibrium vacancy concentration, where $\mu_{Va} = 0$, can be evaluated unambiguously, i.e. there is only one root where $\mu_{Va} = 0$.

2.2. Second method

In this second method, the equilibrium requirement that $\mu_{Va} = 0$ must, of course, be retained, but, instead of the equilibrium vacancy concentration being determined by μ^o_{Va}, this quantity is also set to zero, independent of p, T, or the particular metal or its structure. In other words, the completely empty lattice is selected as the reference state for the vacancies. Adoption of this value results in an equilibrium vacancy concentration of $x_{Va} = 1$ unless an excess Gibbs energy, G^E is introduced. This might be done through the agency of a Redlich–Kister polynomial as, for example, by taking:

$$G^E = Lx_{Va}(1 - x_{Va}) \tag{8}$$

The equilibrium condition, according to this second method, corresponds to:

$$\mu_{Va} = 0 = 0 + RT\log_e x_{Va} + L(1 - x_{Va})^2 \tag{9}$$

An appropriate value for L can be chosen to give exactly the same equilibrium vacancy concentration as obtained from using Eq. (4) as in the first method. There is an

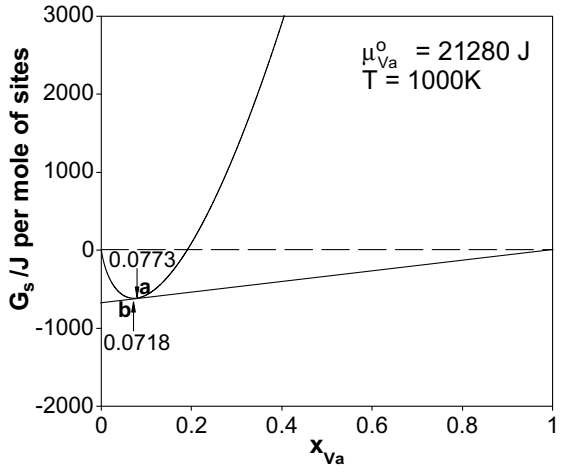

Fig. 4. Gibbs energy per mole of sites vs. vacancy concentration for a pure metal system. The curve has been drawn by assuming that (3) applies and that the equilibrium vacancy concentration is $x_{Va} = 0.0773$, which requires that $\mu^o_{Va} = 21{,}280$ J mol^{-1} at 1000 K.

important difference, however, between the two methods described. In order to obtain a local convex function of G_s with the desired constrained minimum at a low x_{Va} by this second method, it is essential that $L \gg 0$. In the present case, a value of $L = 25{,}000$ J mol^{-1} ($L/RT = 2.36$) has been used in order to obtain the same equilibrium vacancy concentration as obtained by the first method and shown previously in Fig. 4. The selected large positive value of L, however, leads to three possible solution points "**c**", "**d**" and "**e**", which satisfy the condition $\mu_{Va} = 0$, as shown in Fig. 5. Point "**e**" is an unstable state and point "**d**" corresponds to the limiting case as $x_{Va} \to 1$. If the equilibrium condition is being sought via the solution of nonlinear equations rather than from the thermodynamic potential minimum, then the point "**e**", where $\mu_{Va} = 0$, can be found when appropriate starting points are used. In practice, in order to avoid finding either "**d**" or "**e**", an artificial upper bound can be placed on x_{Va} and μ^o_{Va} can be assigned a very small positive value.

Of these two methods used for pure metals, it seems obvious that the first method is to be preferred and is the one usually favored when considering the thermodynamics of vacancies in pure metals (see e.g., [1,2]). The reference state depends on the particular metal and its structure (and on p, T) and it describes uniquely the only available experimental result, the experimental value for the equilibrium vacancy concentration, where $\mu_{Va} = 0$. The second method, on the other hand, uses a reference state that is completely independent of p, T, and the particular metal and its structure and gives three possible solutions for vacancy concentrations where $\mu_{Va} = 0$.

3. Intermediate phases

When vacancies are present in an A–B alloy, it is possible to define different composition variables. For a system A–B–Va:

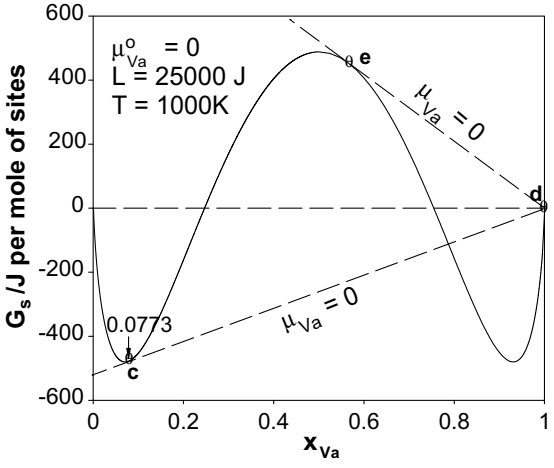

Fig. 5. Gibbs energy per mole of sites vs. vacancy concentration for a pure metal system using (8) for G^E. Three points at "**c**", "**d**" and "**e**", labeled as circles, denote where $\mu_{Va} = 0$.

lattice mole fraction $$x_A = \frac{N_A}{N_A + N_B + N_{Va}} \tag{10}$$

chemical mole fraction $$c_A = \frac{N_A}{N_A + N_B} \tag{11}$$

The total Gibbs energy, given by:

$$G = N_A\mu_A + N_B\mu_B + N_{Va}\mu_{Va} \tag{12}$$

leads to the definition of two different specific Gibbs energies:

$$G_s = \frac{G}{N_A + N_B + N_{Va}} = x_A\mu_A + x_B\mu_B + x_{Va}\mu_{Va} \tag{13}$$

$$G_a = \frac{G}{N_A + N_B} = c_A\mu_A + c_B\mu_B + z\mu_{Va} \tag{14}$$

where the vacancy concentration $z = N_{Va}/(N_A + N_B)$.

3.1. A two-sublattice model

In order to calculate the concentration and distribution of the vacancies and antisite defects, consider a model denoted by:

$$(A, B, Va)_m : (A, B, Va)_n$$

where m and n are the sublattice size fractions, i.e., $m + n = 1$.

The result of minimizing $G([p, T, N_A, N_B], N_{Va})$, for either a disordered (single lattice) phase or an ordered (sublattice) phase, is analogous with that for $G([p, T, N_A], N_{Va})$ in the pure metal case and is given in Eq. (2), i.e.:

$$\left(\frac{\partial G}{\partial N_{Va}}\right)_{p,T,N_A,N_B} = \mu_{Va} = 0 \tag{15}$$

The result from this minimization is the equilibrium total concentration of vacancies (at constant p, T, N_A, N_B), the only experimental result available.

Information about the distribution of the defect species is not available experimentally and can only be calculated via the application of an appropriate model. The modeling equation can be then used in virtual experiments.

Consider a system containing a fixed number of A atoms, N_A and B atoms, N_B which is open to vacancies. The quasi-grand potential,

$$\Omega\left([p, T, N_A, N_B, \mu_{Va}], N_A^{(1)}, N_B^{(1)}, N_{Va}^{(1)}, N_A^{(2)}, N_B^{(2)}, N_{Va}^{(2)}\right)$$

has to be minimized subject to the following mass balance and sublattice size constraints to which are assigned Lagrangian multipliers, λ_i:

$$\left.\begin{aligned} &\lambda_1 \quad N_A - (N_A^{(1)} + N_A^{(2)}) = 0 \\ &\lambda_2 \quad N_B - (N_B^{(1)} + N_B^{(2)}) = 0 \\ &\lambda_3 \quad n\left(N_A^{(1)} + N_B^{(1)} + N_{Va}^{(1)}\right) - m\left(N_A^{(2)} + N_B^{(2)} + N_{Va}^{(2)}\right) = 0 \end{aligned}\right\} \tag{16}$$

The unconstrained Lagrangian, $\mathscr{L}$ is the constrained quasi-grand potential:

$$\mathscr{L} = G - \mu_{Va}^{R}(N_{Va}^{(1)} + N_{Va}^{(2)}) + \lambda_1(N_A - (N_A^{(1)} + N_A^{(2)})) + \lambda_2(N_B - (N_B^{(1)} + N_B^{(2)})) + \lambda_3(n(N_A^{(1)} + N_B^{(1)} + N_{Va}^{(1)}) - m(N_A^{(2)} + N_B^{(2)} + N_{Va}^{(2)})) \quad (17)$$

Differentiation of $\mathscr{L}$ with respect to the various sublattice species amounts gives:

$$\left.\begin{aligned} \mu_A^{(1)} - \lambda_1 + n\lambda_3 &= 0 \\ \mu_B^{(1)} - \lambda_2 + n\lambda_3 &= 0 \\ \mu_{Va}^{(1)} + n\lambda_3 - \mu_{Va}^{R} &= 0 \\ \mu_A^{(2)} - \lambda_1 - m\lambda_3 &= 0 \\ \mu_B^{(2)} - \lambda_2 - m\lambda_3 &= 0 \\ \mu_{Va}^{(2)} - m\lambda_3 - \mu_{Va}^{R} &= 0 \end{aligned}\right\} \quad (18)$$

where the $\mu_P^{(i)}$ are virtual chemical potentials, e.g.:

$$\mu_A^{(1)} = \left(\frac{\partial G}{\partial N_A^{(1)}}\right)_{p,T,N_B^{(1)},N_{Va}^{(1)},N_A^{(2)},N_B^{(2)},N_{Va}^{(2)}}$$

On eliminating the Lagrangian multipliers from Eq. (18), we obtain three independent conditions for the defect equilibria:

$$\mu_{Va}^{R} = m\mu_{Va}^{(1)} + n\mu_{Va}^{(2)} \quad \text{Schottky relation} \quad (19)$$

$$\mu_A^{(1)} + \mu_B^{(2)} = \mu_B^{(1)} + \mu_A^{(2)} \quad \text{Antisite equilm} \quad (20)$$

$$\mu_A^{(1)} = \mu_A^{(2)} + 2\mu_{Va}^{(2)} \quad \text{Triple Defect equilm} \quad (21)$$

The solution of these equations together with the mass and sublattice size ratio constraints provides the answer as to how the species are distributed on the sublattices. It should be emphasized that Eqs. (19–21) apply independent of any particular model used for the energy and entropy representation in the two sublattice model being considered. It is only when such a model is introduced that the virtual chemical potentials for the defect species in these equations can be translated into sublattice concentrations. Fig. 6 was calculated from carrying out such a virtual experiment, the modeling equation in this case being based on the compound energy formalism (CEF).

Using Eq. (15), $\mu_{Va}^{R} = \mu_{Va} = 0$, for the experimentally attainable equilibrium condition, it is seen that this corresponds with:

$$0 = m\mu_{Va}^{(1)} + n\mu_{Va}^{(2)} \quad \text{Schottky equilm} \quad (22)$$

When $m = n = 0.5$, Eq. (22) represents the equilibrium condition for B2 phases, such as B2-AlNi and B2-AlFe. When $m = 1$ and $n \to 0$, it reduces to the equilibrium condition for the single lattice metal–vacancy system.

4. Discussion

The two-sublattice model denoted by:

$$(A, B, Va)_{0.5} : (A, B, Va)_{0.5} \quad (23)$$

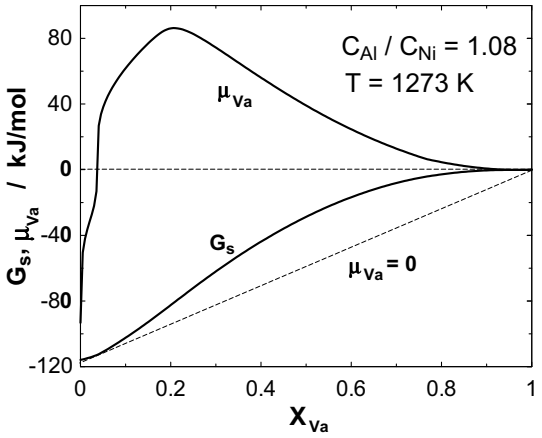

Fig. 6. Application of the standard CEF to the B2 phase in the Al–Ni system [3,4]. There are three values of x_{Va} where $\mu_{Va} = 0$.

has been widely used for describing ordered alloy phases containing significant concentrations of vacancies such as the B2 phase in the Al–Ni system [3,4].

Simpler models than that represented by Eq. (23) have also been used. These include the triple-defect model [5,6] and the hybrid model [7] but all suffer from the serious deficiency that they can never lead to the disordered state. A full Schottky–Wagner treatment of the model given by Eq. (23), in which both antisite and vacancy defects are taken to behave as ideal dilute solutions in the sublattice mole fractions, has been proposed by Krachler et al. [8,9] but this model also suffers from the disadvantage that it can never lead to the disordered phase, since the defect energies are always positive relative to the energies of the major species on each sublattice.

At constant total pressure and temperature, the Gibbs energy of the system denoted by Eq. (23) is a function of the sublattice mole fractions of the sublattice species. A satisfactory model, at least in the Bragg–Williams approximation, must be applicable at any defect concentration and will equally well describe the disordered phase. The CEF [10] has been widely and successfully used for this purpose and is the one concentrated on here.

In the CEF, G_s is written as:

$$G_s = G_s^{\text{ref}} + G_s^{E} + G_s^{\text{id}} \quad (24)$$

The general definition for the reference Gibbs energy, G_s^{ref}, for a two-sublattice model is:

$$G_s^{\text{ref}} = \sum_{i,j}\sum_{P,Q} y_P^i y_Q^j G_{P:Q}^{o} \quad (25)$$

where P, Q are species and i, j are sublattices. The values of $G_{P:Q}^{o}$ in this and the following equations refer to per mole of sites.

For the model represented by Eq. (23), Eq. (25) can be written in full as:

$$\begin{aligned} G_s^{\text{ref}} = {} & y_A^{(1)} y_A^{(2)} G_{A:A}^{o} + y_A^{(1)} y_B^{(2)} G_{A:B}^{o} + y_A^{(1)} y_{Va}^{(2)} G_{A:Va}^{o} \\ & + y_B^{(1)} y_A^{(2)} G_{B:A}^{o} + y_B^{(1)} y_B^{(2)} G_{B:B}^{o} + y_B^{(1)} y_{Va}^{(2)} G_{B:Va}^{o} \\ & + y_{Va}^{(1)} y_A^{(2)} G_{Va:A}^{o} + y_{Va}^{(1)} y_B^{(2)} G_{Va:B}^{o} + y_{Va}^{(1)} y_{Va}^{(2)} G_{Va:Va}^{o} \end{aligned} \quad (26)$$

In this standard CEF treatment of the model represented by Eq. (23), one of the end members is the totally empty lattice, $(Va) : (Va)$, with compound energy $G^o_{Va:Va}$. The only physically realistic selection for the compound energy of such a completely empty end member is zero, independent of temperature, total pressure and host (composition and structure).

The excess Gibbs energy, G^E_s, in Eq. (24) is written in terms of sublattice L parameters. These are similar to the ones used in Eq. (8) for pure metals, except that the contributions to G^E_s are now expressed in terms of the $y^{(i)}_P$. Differences in the ease of vacancy formation on the different sublattices has to be allowed for. This can be achieved by introducing an asymmetry in the metal–vacancy compound energies in Eq. (25), e.g., $G^o_{A:Va}$, and/or by adjusting some of the sublattice L parameter terms in G^E_s.

The last term in Eq. (24), the ideal mixing Gibbs energy, G^{id}_s, is given by the Bragg–Williams expression, which, for the two sublattice model being considered, is given by:

$$G^{id}_s = \frac{1}{2}RT\sum_i\sum_P y^i_P \log_e y^i_P \tag{27}$$

The application of the standard CEF to vacancies in intermediate phases is equivalent to the use of the second method discussed for pure metals. Just as in the pure metal case, a problem arises from the requirement that the principal vacancy property, $G^o_{Va:Va}$, corresponding to a completely empty end member, must be set to zero, independent of temperature, total pressure and host (composition and structure). In turn, this requires that other parameters must be used to explain the observed vacancy concentrations and, in doing so, they are given values which lead to a miscibility gap in the $G_s - x_{Va}$ relation, i.e., there are three roots where $\mu_{Va} = 0$. This is shown in Fig. 3; the results illustrated are from the application of the standard CEF method to the B2-AlNi phase [3,4].

The problem is eliminated if, just as in the use of the first method discussed for pure metals, the ideal dilute solution reference state for $G^o_{Va:Va}$ in the stoichiometric alloy is used. This means that, instead of regarding $(Va):(Va)$ as a completely empty compound end member, it is regarded as a cluster solution member embedded in the host alloy [11]. Just as a single vacancy in a pure metal has an energy and entropy of formation, so do clusters and the same applies in the case of intermetallic compounds. This transformation in the meaning of $(Va):(Va)$ from end member to solution member means that the reference state, $G^o_{Va:Va}$ can be assigned a specific value which depends on temperature, pressure, and the composition and structure of the actual phase being considered.

In the following section, we will illustrate the application of this suggestion towards obtaining a satisfactory description of the thermodynamic properties of B2-AlNi.

4.1. Application to the B2-AlNi phase

From Eq. (26) it can be seen that the only term which can be finite at $x_{Va} = 1$ is $G^o_{Va:Va}$, since this is where $y^{(1)}_{Va} = y^{(2)}_{Va} = 1$ and $y^{(1)}_A = y^{(2)}_A = y^{(1)}_B = y^{(2)}_B = 0$. However, the other terms in Eq. (26) which contain vacancy concentrations are important at compositions where $x_{Va} \neq 1$. As a result, unlike the analogous pure metal case, it is not possible to assign a unique value to $G^o_{Va:Va}$. One obvious way around this problem is to assign a value to this quantity corresponding to the equilibrium at the stoichiometric composition

$$0 = G^o_{Va:Va} + RT\log_e(x^{eq}_{Va}) \tag{28}$$

where $G^o_{Va:Va}$ refers to the ideal dilute solution reference state.

Eq. (28) has been used in the construction of Fig. 7 for stoichiometric AlFe [12] and AlNi [13]. It can be seen that, whilst the values of $G^o_{Va:Va}$ calculated in this way are approximately temperature independent, they depend on the particular host and conditions. It is this dependence which results in a problem for the application of this method to multicomponent solutions. In the case of the ternary B2-AlFeNi phase, which in our two sublattice model is represented by:

$$(Fe, Ni, Al, Va) : (Fe, Ni, Al, Va)$$

one would like to obtain $G^o_{Va:Va}$ in the multicomponent alloy by using an interpolation equation such as:

$$G^o_{Va:Va}[Al_{0.5}(Fe,Ni)_{0.5}] = \left(\frac{c_{Fe}}{c_{Fe}+c_{Ni}}\right)G^o_{Va:Va}[Al_{0.5}(Fe)_{0.5}] + \left(\frac{c_{Ni}}{c_{Fe}+c_{Ni}}\right)G^o_{Va:Va}[Al_{0.5}(Ni)_{0.5}]$$

The presently available software, however, does not allow for such an interpolation. Given this situation, it seems that the simplest way is to select one particular value for $G^o_{Va:Va}$ and use it in all circumstances. As long as this value is sufficiently large and positive, it will ensure that there is only one vacancy concentration where $\mu_{Va} = 0$. We have selected a temperature-independent value of $G^o_{Va:Va} = 60$ kJ mol^{-1}, corresponding to its approximate value for B2-AlNi.

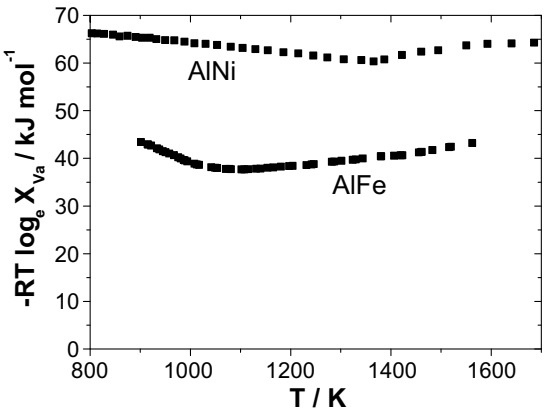

Fig. 7. $G^o_{Va:Va}$ for the ideal dilute solution reference state as a function of temperature in stoichiometric B2-AlNi. The vacancy concentration results are taken from Scholz [13] and Pike et al. [14].

The basis of the calculation was to accept the thermodynamic description given by Dupin et al. [3,4] for all phases except the B2 phase. The experimental results used in the optimization for the B2 phase were identical to those used by Dupin et al. [3,4], except that the more recent results of vacancy concentration measurements of Pike et al. [14] and Scholz [13] were used. Other recent experimental results, unavailable to Dupin et al., were not used in the present optimization since the aim was limited to demonstrating the use of the ideal dilute reference state for vacancies. The results from a detailed optimization using the most recently available experimental results will be given in a subsequent communication devoted to the Al–Fe–Ni system. Parameter optimization was carried out using PanOptimizer [15].

The effects of using $G^{o}_{Va:Va} = 60$ kJ mol^{-1} are shown in Fig. 8, where it can be seen that there is now only one vacancy concentration where $\mu_{Va} = 0$.

Figs. 9–11 show comparisons between the calculated and experimental phase diagrams [17–25], enthalpies of formation at 1100 K [16], and the vacancy concentrations

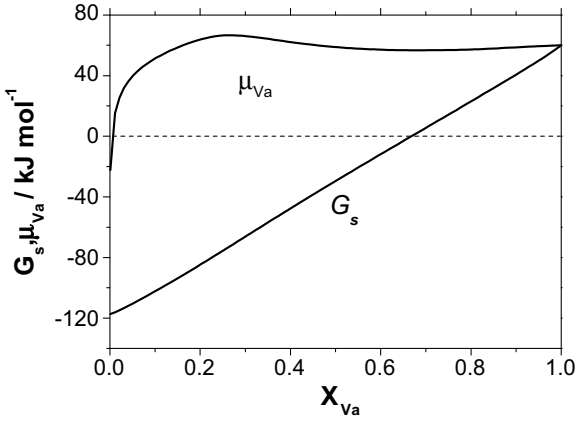

Fig. 8. Gibbs energy per mole of sites and chemical potential of vacancies vs. vacancy concentration in stoichiometric B2-AlNi at 1273 K using the ideal dilute solution reference state for $G^{o}_{Va:Va}$.

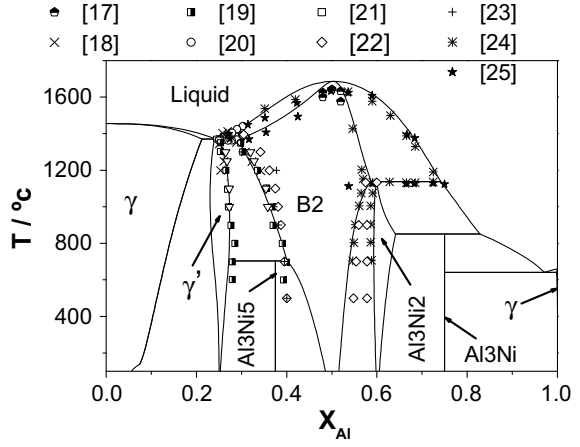

Fig. 9. Comparison of the calculated and experimental [17–25] phase diagram in the region containing the B2-AlNi phase.

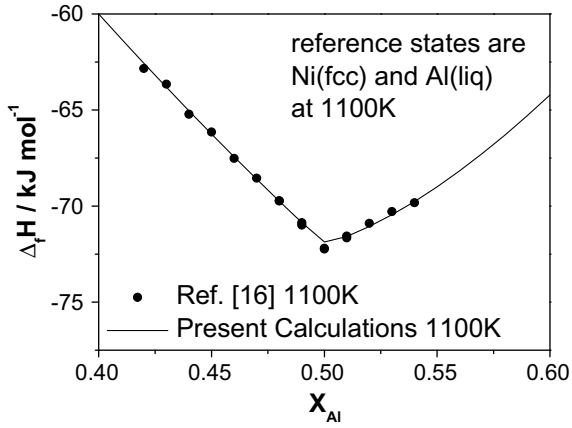

Fig. 10. Comparison of the calculated and experimental [16] enthalpies of formation for B2-AlNi at 1100 K.

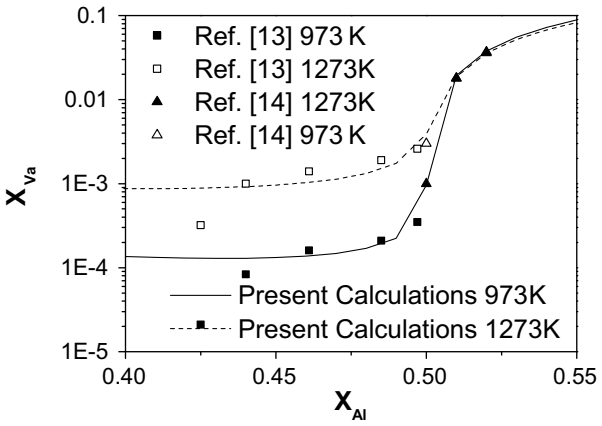

Fig. 11. Comparison of the calculated and experimental [13,14] vacancy concentrations for B2-AlNi as a function of composition at 973 and 1273 K.

at 973 and 1273 K [14,13]. In all cases, it can be seen that the agreement is extremely good. The number of parameters required in order to obtain this good description of the B2 phase is fewer than used by Dupin et al. [3,4] in their original description using $G^{o}_{Va:Va} = 0$. The phase diagram calculated by Dupin et al. [3,4] is in better agreement with experimental results for the liquid/B2 phase equilibrium than those presented in Fig. 9, but this is because we have accepted their description for the liquid phase. In a complete reoptimization of the properties for all the phases in the system these differences would not be apparent.

5. Conclusions

In the standard application of the CEF to intermediate phases containing vacancies, it is necessary to assume that $G^{o}_{Va:Va} = 0$ for the end member $(Va):(Va)$ if the formalism is to have any physical meaning. This approach means, however, that this important vacancy property is assumed independent of pressure, temperature, chemical composition or structure of the phase involved. The assumption always leads to three vacancy concentrations where $\mu_{Va} = 0$ or,

equivalently, to the formation of a miscibility gap in the Gibbs energy as function of the vacancy concentration.

We have suggested that, by using the infinitely dilute solution reference state for $G^{o}_{Va:Va}$, which is the preferred method for treating the thermodynamics of vacancies in pure metals, the CEF can be adapted to the intermediate phase case. It requires viewing $(Va):(Va)$ as being a solution member rather than as being a compound end member. Not only is this modification more satisfactory physically, it also avoids the multiple root problem for the equilibrium condition $\mu_{Va} = 0$.

The application of this strategy for handling vacancies in the ternary Al–Fe–Ni system will be considered in a future publication.

Acknowledgements

Y.A.C. wishes to acknowledge the financial support of AFOSR (FA9550-06-1-0229) and Drs. Brett P. Conner and J. Tiley, Program Managers for this program for their interest in this work. E.D. and R.S.F. wish to thank the German Research Foundation (DFG) for support under Grant No. Schm 588/31.

References

[1] Cahn RW, Haasen P. Physical metallurgy. Amsterdam: North-Holland; 1980.
[2] Allnatt AR, Lidiard AB. Atomic transport in solids. Cambridge: Cambridge University Press; 1993.
[3] Dupin N, Ansara I. Z Metallkd 1999;90(1):76–85.
[4] Dupin N, Ansara I, Sundman B. CALPHAD 2001;25:279–98.
[5] Chang YA, Neumann JP. Prog Solid State Chem 1982;14:221–301.
[6] Ansara I, Dupin N, Lukas HL, Sundman B. J Alloys Comp 1997:20–30.
[7] Ren X, Otsuka K. Philos Mag A 2000;80(2):467–91.
[8] Krachler R, Ipser H, Komarek KL. J Phys Chem Solids 1989;50(11):1127–35.
[9] Krachler R, Ipser H. Intermetallics 1999;7(2):141–51.
[10] Hillert M. J Alloys Comp 2001;320(2):161–76.
[11] Oates WA. Int J Mater Res 2007;9:780–5.
[12] Wolff J, Franz M, Broska A, Kerl R, Weinhagen M, Köhler B, et al. Intermetallics 1999;7:289–300.
[13] H.P. Scholz, Messungen der absoluten leerstellenkonzentration in nickel und geordneten intermetallischen nickel-legierungen mit einem differentialdilatometer, Ph.D. thesis, University of Göttingen, Germany (2001).
[14] Pike LM, Anderson IM, Liu CT, Chang YA. Acta Mater 2002;50:3859–79.
[15] PANDAT™ Software for Multicomponent Phase Diagram Calculation, Computherm LLC, 437 S. Yellowstone Drive, Suite 217, Madison, WI 53719, USA.
[16] Henig E, Lukas HL. Z Metallkd 1975;66:98–108.
[17] Cotton JD, Noebe RD, Kaufmann MJ. J Phase Equilib 1993;14(5):579–82.
[18] Verhoeven JD, Lee JH, Laabs FC, Jones LL. J Phase Equilib 1991;12(1):15–23.
[19] C.D. Jia, Ph.D. thesis, Tohoku University, Sendai, Japan (1990).
[20] Bremer FJ, Beyss M, Karthaus E, Hellwig A, Schober T, Welter JM, et al. J Crystal Growth 1988;87(2-3):185–92.
[21] Hilpert K, Kobertz D, Venugopal V, Miller M, Gerads H, Bremer FJ, et al. Z Naturforsch Teil A 1987;42:1327–32.
[22] Taylor A, Doyle NJ. J Appl Crystallogr 1972;5:201–9.
[23] Schramm J. Z Metallkd 1941;33:355–74.
[24] Alexander WO, Vaughan NB. J Inst Met 1973;61:247–348.
[25] Gwyer AGC. Z Anorg Chem 1908;57:113–26.